Published in final edited form as:
Alzheimer Dis Assoc Disord. 2006 ; 20(2): 77–85.

Effects of Alzheimer Disease on Fronto-parietal Brain *N*-acetyl Aspartate and Myo-Inositol Using Magnetic Resonance Spectroscopic Imaging

Xiaoping Zhu, MD, PhD[*,†], **Norbert Schuff, PhD**[*,†], **John Kornak, PhD**[*,†,‡], **Brian Soher, PhD**[§], **Kristine Yaffe, MD**[||], **Joel H. Kramer, PsyD**[||], **Frank Ezekiel, BA**[*,†], **Bruce L. Miller, MD**[¶], **William J. Jagust, MD**[#], and **Michael W. Weiner**[*,||,†,¶]

* *Department of Radiology, VA Medical Center*

|| *Department of Psychiatry, VA Medical Center*

† *Department of Radiology, University of California, San Francisco*

‡ *Department of Epidemiology and Biostatistics, University of California, San Francisco*

¶ *Department of Neurology, University of California, San Francisco*

Department of Radiology, UC Berkeley, Berkeley, CA

§ *Duke Center for Advanced MR Development, Duke University Medical Center, Durham, NC*

Abstract

Previous magnetic resonance (MR) spectroscopy studies of Alzheimer disease (AD) reporting reduced *N*-acetyl aspartate (NAA) and increased myo-Inositol (mI) used single voxel techniques, which have limited ability to assess the regional distribution of the metabolite abnormalities. The objective of this study was to determine the regional distribution of NAA and mI alterations in AD by using MR spectroscopic imaging. Fourteen patients with AD and 22 cognitively normal elderly were studied using structural MR imaging and MR spectroscopic imaging. Changes of NAA, mI, and various metabolite ratios were measured in frontal and parietal lobe gray matter (GM) and white matter. This study found: (1) when compared with cognitively normal subjects, AD patients had increased mI and mI/creatine (Cr) ratios primarily in parietal lobe GM, whereas frontal lobe GM and white matter were spared; (2) in the same region where mI was increased, AD patients had also decreased NAA and NAA/Cr ratios, replicating previous findings; (3) however, increased mI or mI/Cr ratios did not correlate with decreased NAA or NAA/Cr ratios; and (4) using mI/Cr and NAA/Cr together improved sensitivity and specificity to AD from control as compared with NAA/Cr alone. In conclusion, decreased NAA and increased mI in AD are primarily localized in parietal lobe GM regions. However, the NAA and mI changes are not correlated with each other, suggesting that they represent different processes that might help staging of AD.

Keywords

Alzheimer disease; short TE 1H magnetic resonance spectroscopic imaging; brain myo-Inositol

Reprints: Xiaoping Zhu, MD, PhD, MR Unit, 114M, VA Medical Center/UCSF, 4150 Clement Street, San Francisco, CA 94121 (e-mail: zhupxia@itsa.ucsf.edu)..

Sources of Support: Grant sponsor: NIH; Grant numbers: AG10897; AG12435; EB00207; EB00822; EB000766; Grant sponsor: VA Research: MIRECC, REAP.

Alzheimer disease (AD) is characterized by accumulation of intraneuronal neurofibrillary tangles and extracellular amyloid plaques, as well as progressive loss of neurons that initially involve the hippocampal formation, temporoparietal cortex, and at later stages other cortical regions.[1–3] Such stereotypical regional spread of pathology may be delineated with imaging techniques, including structural magnetic resonance imaging (MRI), which showed brain tissue loss[4] and functional imaging by positron emission tomography (PET), which demonstrated cerebral glucose hypometabolism in AD.[5] However, neither structural MRI nor PET provides specific measures of neuronal or glial alterations.

In vivo 1H magnetic resonance spectroscopy (MRS) has been used to measure levels of brain metabolites, such as *N*-acetyl aspartate (NAA) and myo-Inositol (mI) in AD.[6] Because NAA is found in relatively high concentration in neuronal tissue and its processes but is virtually undetectable in other tissue, including glia,[7] a decline of NAA is usually interpreted as marker of neuronal or axonal loss or dysfunction.[8,9] Many single voxel (SV) MRS and multivoxel magnetic resonance spectroscopic imaging (MRSI) studies have shown reduced NAA in AD, especially in hippocampus and parietal lobe, with lesser reductions in frontal lobe.[10,11]

mI has been suggested as a glial marker[12,13] and, in contrast to NAA, is increased in AD.[14,15] Many SV MRS studies showed increased mI[16–23] associated with decreased NAA[16–20,23–26] in AD. However, SV MRS has limited ability to measure regional metabolite variations and thus, the regional distribution of mI elevations in AD remains unclear. Furthermore, the effect of gray matter (GM) and white matter (WM) partial volume on mI alterations is difficult to eliminate with SV MRS. MRSI techniques,[27,28] which provide regional maps of metabolites, have the advantage over SV MRS in that spectra are obtained from multiple small voxels over a large field of view, sampling regions of both GM and WM. However, MRSI studies of mI have been technically challenging because of the short transverse relaxation time of mI. Few MRSI studies with short TE have been reported that studied the distribution of mI changes in patients with multiple sclerosis,[29] epilepsy,[30,31] chronic alcohol-induced brain damage,[32] and cerebral autosomal dominant arteriopathy with subcortical infarcts and leukoencephalopathy. [33] However, most MRSI studies of AD were performed at long echo time,[10,34–38] which does not accomplish detection of mI. To our knowledge, there has been no previous short TE MRSI report on regional mI alterations in AD.

Recently, we developed a new data processing strategy to improve measurement reliability of short TE MRSI data that incorporates computation of regional coherent mean spectra (RCMS) with high signal-to-noise ratio and reduced baseline fluctuations.[39,40] In the present study, we used RCMS to determine regional and gray/white matter variations of mI and other metabolites, including NAA, and creatine (Cr) in AD and in cognitively normal (CN) elderly subjects.

The overall goal of this study was to determine the regional pattern of altered mI and NAA in AD compared with CN. Specifically, our aims were (1) to test the hypothesis that mI is primarily elevated in parietal GM regions in AD, similar to the previously reported regional pattern of NAA loss in AD,[10] (2) to replicate previous findings of selective NAA reduction of parietal GM in AD, (3) to determine if the elevated mI and NAA alterations in parietal lobe GM in AD are correlated, and (4) to explore whether measurement of mI improves classification of AD from CN over that using NAA measures alone.

METHODS

Subjects

Using MRSI, regional NAA and mI concentrations and their ratios, that is, NAA/Cr, mI/Cr, and NAA/mI were measured in 14 patients with a clinical diagnosis of AD and 22 CN elderly

subjects who participated in this study. The AD patients (6 men, 8 women, mean age 73.0±6.2 y) were recruited from the Memory and Aging Center of the University of California, San Francisco and the Alzheimer Center at the University of California, Davis and received the standard battery of cognitive and neuropsychologic tests in the referral centers.[41] A clinical diagnosis of probable AD was established according to the National Institute of Neurological and Communicative Disorders and Stroke-Alzheimer's Disease and Related Disorders Association (NINCDS-ADRA) criteria. [42] AD patients had Mini-Mental State Examination (MMSE)[43] scores of 20.0±6. The CN subjects (9 men, 13 women, mean age 72.1±8.5 y) were recruited from the community and received standard neuropsychologic examinations at the same referral centers. CN subjects had MMSE scores of 29.7±0.5. None of the included subject had a clinical history of psychiatric illness epilepsy, hypertension, diabetes, major heart disease, head trauma, or alcoholism. In addition, a neuroradiologist evaluated the MRI data of all subjects to exclude major neuropathologies other than AD. All subjects or their legal guardians gave voluntarily written informed consent, approved by the Committees of Human Research at the University of California in San Francisco and Davis and the VA Medical Center in San Francisco, before participating in the study.

Data Acquisition

MRSI was performed on a 1.5 T MR scanner (Vision, Siemens Medical Systems, Iselin, NJ) using a multislice MRSI sequence with a short spin-echo time of 25 ms and lipid signal nulling by slice selective inversion recovery, as described in detail earlier.[44] Three axial oblique MRSI slices, each 15mm thick and with a nominal in-plane resolution of $7.5 \times 7.5 mm^2$, were acquired. Voxels outside the brain were discarded for analysis to minimize contamination from nonbrain tissue by applying a brain tissue mask to each in vivo MRSI data set, using information from tissue segmented high spatial resolution MRI data, aligned to MRSI.

Data Postprocessing

All processing steps of 1H MRSI were fully automated, avoiding rater bias. To reduce lipid contamination of the metabolite spectra, a fully automated procedure to detect extracranial lipid regions was used together with an iterative method for selective *k*-space extrapolation of lipid resonances.[45] Automated fitting of NAA, Cr, and mI and baseline correction was performed using software that incorporated prior spectral knowledge in the fitting procedure. [46] To eliminate instrumental variations between subject scans, metabolite intensities were normalized to the intensity of ventricular cerebrospinal fluid (CSF) signal of each subject on proton density-weighted MRI with adjustments for receiver gain and coil loading variations.

To obtain metabolite concentrations at different regions in the brain, as shown in Figure 1, the tissue compositions of the 1H MRSI voxels were estimated by incorporating the segmented MRI data (Fig. 1A) into the analysis of 1H MRSI data (Fig. 1B). MRI processing consisted of tissue segmentation using semiautomated methods on a slice-by-slice basis for separation of brain into CSF, GM, and WM[47] on the high spatial resolution MRI. Manual tracing was used to outline the main brain lobes,[48,49] such as frontal, parietal, temporal, and occipital lobes. Figure 1 also shows the slice position of MRSI and MRI (Fig. 1C). A contour plot overlaid with the NAA image demonstrates the alignment between MRSI and MRI data (Fig. 1D). Voxels containing more than 30% CSF or 10% WM hyperintensities (WMH) were excluded from the analysis to obtain spectra covering primarily GM and normal WM tissue. Spectra from the remaining voxels within each region of interest (frontal and parietal lobe GM and WM) were then coherently combined after the RCMS approach. Details of the computation of RCMS spectra, which take phase and frequency variations of the spectra into account, are described in Refs. 39, [40]. Areas under each spectral line, for example NAA, Cr, and mI, in the RCMS spectra were then calculated by applying the automated fitting program.[46]

Statistical Analysis

Metabolite variations were modeled as a function of diagnosis and brain region using a linear mixed-effect (LME) model[50] (Splus 7, Insightful, Seattle, and R, Copyright 2004, The R Foundation for Statistical Computing Version 2.0.1) with subject specific random effects and fixed region effects. Multivariate responses of the individual metabolite levels were defined across the 3 regions being investigated to incorporate some correction for family-wise multiple comparison error. Tissue fractions of GM or WM, defined as *tissue fraction (TF)* $=V_{\text{GM or WM}}/(\textit{total volume})100\%$, were included in the model as a linear fixed covariate to account for tissue-dependent metabolite variations. $V_{\text{GM or WM}}$ denotes % volume of either GM or WM obtained from segmentation on high spatial resolution MRI and *total volume* is the sum of GM, WM, and CSF.

Age and WMH were also included as linear fixed covariates to account for their variations. An unstructured covariance matrix was adopted for the within-subject relationship of the 3 regions of interest. Homogeneous and independent error variance was imposed on the individual groups. χ^2 likelihood ratio tests were used to determine the existence of significant variance differences between groups (the grouping variables and other covariates were included at this stage). However, the AD and CN groups were fitted allowing for different magnitudes of error variance, because likelihood ratio tests consistently showed that the variability in the AD group was significantly different from that of the CN group. This LME model was fit via maximum likelihood and conditional *t* tests were used to determine whether diagnosis was an important explanatory variable in the model. Metabolites for which diagnosis contributed significantly to the multiregion model were examined further for the presence of individual region effects. A significance level of 0.05 was used for all tests. LME modeling was also used to fit variations of hippocampal or GM volumes measured using structural MRI as a function of diagnosis with adjustments for age and WMH load.

Spearman rank correlation coefficients were used to examine relationships between NAA and mI, and between NAA/Cr and mI/Cr in different brain regions and in different tissue types (GM or WM). The same tests were used to examine relationships between changes in metabolite measurements and MMSE scores.

A receiver operator characteristics analysis was used to evaluate the classification of subjects as AD or CN. The area under the curve (AUC) was evaluated by bootstrapping the logistic regression model. Further, to avoid over-fitting, a leave-one-out classification procedure was performed using logistic regression analysis for the following explanatory variables and combinations: NAA/Cr, NAA/Cr plus mI/Cr, and NAA/mI. Furthermore, the classifications from the use of metabolite measurements were compared with those from hippocampal volume measurements, which are generally considered a sensitivity imaging marker for AD.[48] Finally, we tested the performance of combinations of spectroscopy and volumetric measures.

RESULTS

Demographics, Clinical Data

Table 1 lists the demographics and clinical data of the study groups. The groups were similar in distribution of age (P=0.60, 2-sided *t* test) and sex (P=0.81, Pearson χ^2 test). In addition, WMH volumes were not significantly different between CN and AD (P=0.28, 2- sided *t* test). As expected, AD had markedly lower MMSE scores, indicating greater cognitive impairment, than that of CN (P<0.0001, 2-sided Wilcoxon test).

Comparison of MRI Volumes Between AD and CN Using LME

The MRI-derived structural differences between the groups of hippocampus and cortical GM volumes and the conditional *t* test *P* values from the LME model fits are listed in Table 2. In agreement with many other MRI studies,[51,52] AD had smaller hippocampi (22.0% in the left; 22.2% in the right, $P<0.0001$ for both), and less cortical GM (7.1%, $P=0.0002$) and WM (5.0%, $P=0.02$) volumes than CN after accounting for age, WMH, and TF.

Figure 2 shows representative metabolite images of mI and NAA as well as representative RCMS of parietal GM in a 66-year-old patient with AD and an 85-year-old CN subject. The RCMS spectra show that the patient presented elevated mI and reduced NAA compared to the CN subject.

Comparison of mI, NAA, and Metabolite Ratios Between AD and CN

Table 3 shows metabolic concentrations of mI and NAA, and the ratios of mI/Cr, NAA/Cr, and NAA/mI of parietal GM, frontal GM, parietal WM, and frontal WM in AD and CN. Conditional *t* test *P* values for multivariate analysis of covariance are also listed. After accounting for age, WMH, and variations in the amount of tissue fractions in the MRSI voxels, AD patients had overall greater mI (10%, $P=0.048$) and a greater mI/Cr ratio (9.8%, $P=0.07$) in parietal lobe GM than those of CN subjects. mI alterations in frontal lobe GM (16.7%) and parietal lobe WM (8.2%) in AD were not significant ($P=0.40$ and 0.26). In contrast to mI, AD patients had less NAA (10%, $P=0.044$), a smaller NAA/Cr ratio (11%, $P=0.0009$), and a smaller NAA/mI ratio (18.5%, $P=0.0003$) in parietal lobe GM than those of CN subjects, whereas in frontal lobe GM no significant differences of NAA or NAA/mI were found. However, NAA/Cr of frontal lobe GM was reduced in AD (8.6%, $P=0.006$) compared with CN subjects. In addition to the alterations in GM, AD patients had smaller NAA/Cr ratios (7.4%, $P=0.02$) and smaller NAA/mI ratios (11%, $P=0.03$) in parietal lobe WM than CN subjects. In frontal lobe WM, no significant metabolite differences between AD and CN were detected. Cr levels were similar in AD and CN.

Regional Differences

Regional variations of reduced mI and NAA in AD were not significant. However, the reductions of NAA/mI in AD were larger in parietal lobe GM than in each of frontal lobe GM ($P=0.056$), parietal lobe WM ($P=0.034$), and frontal lobe WM ($P<0.0001$).

Correlations of NAA With mI in AD

In parietal lobe GM of AD, increased mI was not significantly correlated with decreased NAA ($r=0.36$, $P=0.20$) and increased mI/Cr was not correlated with decreased NAA/Cr ($r=0.18$, $P=0.53$), as shown in Figure 3. In frontal GM of AD, however, NAA and mI were weakly correlated ($r=0.58$, $P=0.04$), but significance was lost after correction for multiple comparisons. No correlations were found between NAA and mI in other brain regions.

Correlation of MMSE With Metabolites

We tested whether dementia severity, as assessed using MMSE, correlated with metabolite measures in AD. MMSE scores correlated with NAA/Cr in parietal GM ($r=0.57$, $P=0.04$), but significance was lost after correction for multiple comparisons. No other significant correlations between MMSE and NAA, mI, or mI/Cr ratios were found.

Classification of AD From CN

Finally, we tested the extent to which mI measures improved classification of AD and CN as compared with that based on NAA measures alone. Table 4 lists the sensitivity, specificity, and overall correct classification of AD and CN for these combinations. Table 4 also lists

particular *P* values calculated from the logistic regression analysis, whereas the explanatory variables and covariates were estimated together using the general linear regression model. Results show that mI/Cr ratios made significant contributions to the classification. For the model with only NAA/Cr in parietal GM as an explanatory variable, prediction of group membership was significant (P=0.01), yielding an AUC of 0.81. The addition of mI/Cr as a covariate in the logistic regression model led to a significant increase of the AUC to 0.90 with P=0.01 and 0.039 from NAA/Cr and mI/Cr, respectively. The leave-one-out test revealed an improved overall classification of 78% with a sensitivity of 64% and specificity of 86%. The NAA/mI ratios yielded an overall classification of 75% with a sensitivity of 57% and specificity of 86%. In comparison, hippocampal volumes yielded an overall classification of 81%, slightly higher than NAA/Cr and mI/Cr taken together. The best classification was achieved by including the NAA/mI and hippocampal volume, when 89% of cases were classified correctly.

DISCUSSION

This study measured the regional distribution of mI and other major brain metabolites using spectroscopic imaging. In addition, alterations of metabolites in GM and WM were differentiated using the regionally coherent mean spectra approach.[39,40] In contrast, previous studies of mI abnormalities in AD used SV MRS methods that permit only limited assessment of regional variations. Furthermore, differentiating between WM and GM metabolite changes is difficult with SV MRS, because of inevitable partial volume effects.

The major findings are the following: (1) when compared with CN subjects, AD patients had significantly increased mI and mI/Cr ratios in parietal lobe GM, but no significant changes in frontal lobe GM, parietal lobe WM, or frontal lobe WM; (2) NAA and NAA/Cr ratios were reduced in AD in parietal lobe GM matter, replicating previous findings; (3) the reductions of NAA/mI in AD were larger in parietal lobe GM than in each of frontal lobe GM, parietal lobe WM, and frontal lobe WM; (4) in AD, increased mI (or mI/Cr) did not correlate with decreased NAA (or NAA/Cr), despite the observation that mI and NAA alterations occurred in the same brain region—this finding is consistent with the view that changes of these metabolites represent different pathologic processes; and (5) measurements of mI/Cr and NAA/mI ratios improved classification of AD from CN, and the best classification was achieved by including parietal lobe NAA/mI and hippocampal volume. Taken together, the results emphasize the value of mI for evaluation of AD.

Increased mI in Parietal GM of AD

The finding that increased mI occurs primarily in parietal lobe GM of AD compared with controls is similar to previous findings of reduced NAA in this same region[53] and is consistent with many pathologic and PET studies that the parietal lobe is a major site of AD pathology. However, it was not possible to obtain reliable metabolite data from medial temporal lobe or temporal cortex, because of difficulties to achieve sufficiently magnetic field homogeneity in this region, resulting in broader metabolite signals, poor water suppression, and inability to accurately measure metabolite values. MR spectroscopy studies of the median temporal lobe are currently more reliable with SV MRS, such as the point resolved spectroscopy sequence[21] or the stimulated-echo acquisition mode[54] techniques, which specifically target this region and permit localized shimming.

Increased mI and mI/Cr ratios were reported previously in brain regions of occipital,[16,17] posterior cingulated,[18–20] frontal,[21,22] parietal,[16,21] and paratrigonal WM.[23] Many reported increases of mI or mI/Cr ratio coexisted with decreases of NAA or NAA/Cr ratio,[16–18,23–26] and increases of mI/H_2O ratio coexisted with decreases of NAA/H_2O ratio.[22] Fewer reported increases of mI and mI/Cr ratios but with no change of NAA,[21,55] or decreases of NAA and NAA/Cr ratios but no changes of mI and mI/Cr ratios in AD.[56] One study[57]

found no statistically significant alterations of mI, NAA, or metabolite ratios, between AD and CN.

mI is present in glial cells but not in neuronal cell cultures.[13] An increase in mI might therefore reflect glial activation or proliferation, accompanying neuronal dysfunction or loss.[58,59] mI has been shown to be an organic osmolyte in neuroglial cells with a function of maintaining cell volume[60] when neuron loss is prominent. One SV MRS study found elevated mI levels in mild cognitively impaired subjects, who are at increased risk for AD, in the absence of NAA changes, implying that glial changes may precede neuronal changes.[19]

Consistent with previous observations,[61,62] we found metabolite ratios had less variations than absolute concentrations despite careful adjustments of signal intensities for receiver gain variations between subject and normalization to the CSF water signal from MRI.[63] This suggests that the larger variability of concentrations cannot be explained by technical imperfections alone. Although there were no significant differences in Cr across groups, the normalization to Cr may have compensated for regional variations in metabolite concentrations between subjects, resulting overall in less variability of ratios than concentrations. Whether AD is associated with larger regional variability of metabolite concentrations within a subject could not conclusively be determined because statistical power was limited in this study owing to the small number of subjects.

Correlations Between mI and NAA

Our a priori hypothesis was that there would be significant correlations between NAA (which decreases in AD) and mI (which increases in AD) based on the concept that neuronal dysfunction or loss in AD might be accompanied by glial activation or proliferation. We found no significant correlations between NAA and mI or NAA/Cr and mI/Cr ratios, despite the observation that mI and NAA changes appeared in the same brain region. These findings, contracting our a priori hypothesis, suggest a disassociation between mI and NAA alterations in AD. This has also been observed by previous investigators.[22] A possible explanation for the lack of such correlations is that NAA largely reflects changes in neuronal cell bodies, especially in GM, whereas mI largely reflects change in glial cells, which are more widely distributed in WM.[16,23]

Value of Using mI and NAA for Classification

We found improved classification between AD and CN when mI/Cr ratios were used together with NAA/Cr ratios. The results replicate and extend previous SV MRS reports demonstrating the added value of measuring mI together with NAA.[12,16,18,21,24,55,64] The combined NAA/Cr and mI/Cr in parietal lobe GM by short TE 1H MRSI yielded a modest predictive value for distinguishing AD from normal subjects. In comparison, other 1H MRS studies reported classification rates ranging from 68% to 90%[10,24,47,65–68] (Table 5). The combination of spectroscopic findings in parietal lobe GM and volumetric measures of hippocampus resulted in the largest group separation between AD and CN with an overall classification of 89%. However, because the diagnosis of probable AD was clinically determined and not confirmed by autopsy, the value in taking MRSI and MRI measures together cannot conclusively be determined. More precise estimation of diagnostic accuracy may require to be performed on those probable AD with histologic verifications. [52]

Limitations

Because the small AD sample in this study included patients with advanced dementia, the findings do not shed light on early diagnostic indicators. Prospective studies on nondemented subjects, who eventually convert to AD, are necessary to determine if the metabolite abnormalities are indicators of incipient AD.

Another limitation of this study is that the spectra could not be acquired from the entire brain, especially from temporal lobe regions (an important site for AD). This was due to the aforementioned problems of poor shimming and poor water suppression in the temporal lobe regions. It, therefore, remains unclear whether lack of a correlation between NAA and mI in AD is a global feature or limited to parietal lobe regions. Furthermore, even though the 1H MRSI voxels used in the current size were considerably smaller than voxels used in SV MRS, some MRSI voxels still contained mixtures of GM, WM, and CSF. Although we accounted for these effects in the statistical model, we cannot rule out the possibility of that some bias towards tissue coverage was introduced, because very healthy subjects usually have more GM left than patients in advanced stages of AD.

CONCLUSIONS

The observation of increased mI in primarily parietal lobe GM regions in AD is consistent with the known distribution of AD pathology. Furthermore, lack of a correlation between increased mI and decreased NAA in this region suggests that mI and NAA reflect different pathologic processes and may explain improved classification of AD from CN when mI/Cr and NAA/Cr ratios are used together.

Acknowledgements

The authors thank Diana Sacrey, Meera Krishnan, Marybeth Kedzior, and Shannon Buckley for MRI and MRSI scanning of the elderly subjects and patients, Dawn Hardin for measuring hippocampal volumes. They also thank Dr Ying Lu for useful discussion on receiver operator characteristics analysis.

References

1. Braak H, Braak E. Neuropathological stageing of Alzheimer-related changes. Acta Neuropathol (Berlin) 1991;82:239–259.
2. Braak E, Braak H. Alzheimer's disease: transiently developing dendritic changes in pyramidal cells of sector CA1 of the Ammon's horn. Acta Neuropathol (Berlin) 1997;93:323–325.
3. Lee BC, Mintun M, Buckner RL, et al. Imaging of Alzheimer's disease. J Neuroimaging 2003;13:199–214. [PubMed: 12889165]
4. Du AT, Schuff N, Zhu XP, et al. Atrophy rates of entorhinal cortex in AD and normal aging. Neurology 2003;60:481–486. [PubMed: 12578931]
5. Hoffman JM, Welsh-Bohmer KA, Hanson M, et al. FDG PET imaging in patients with pathologically verified dementia. J Nucl Med 2000;41:1920–1928. [PubMed: 11079505]
6. Valenzuela MJ, Sachdev P. Magnetic resonance spectroscopy in AD. Neurology 2001;56:592–598. [PubMed: 11261442]
7. Bates TE, Strangward M, Keelan J, et al. Inhibition of N-acetyl aspartate production: implications for 1H MRS studies in vivo. Neuroreport 1996;7:1397–1400. [PubMed: 8856684]
8. Birken DL, Oldendorf WH. N-acetyl-L-aspartic acid: a literature review of a compound prominent in 1H-NMR spectroscopic studies of brain. Neurosci Biobehav Rev 1989;13:23–31. [PubMed: 2671831]
9. Griffin JL, Bollard M, Nicholson JK, et al. Spectral profiles of cultured neuronal and glial cells derived from HRMAS (1)H NMR spectroscopy. NMR Biomed 2002;15:375–384. [PubMed: 12357551]
10. Schu N, Capizzano AA, Du AT, et al. Selective reduction of N-acetyl aspartate in medial temporal and parietal lobes in AD. Neurology 2002;58:928–935. [PubMed: 11914410]
11. Hsu YY, Du AT, Schuff N, et al. Magnetic resonance imaging and magnetic resonance spectroscopy in dementias. J Geriatr Psychiatry Neurol 2001;14:145–166. [PubMed: 11563438]
12. Ross BD, Bluml S, Cowan R, et al. In vivo MR spectroscopy of human dementia. Neuroimaging Clin N Am 1998;8:809–822. [PubMed: 9769343]
13. Brand A, Richter-Landsberg C, Leibfritz D. Multinuclear NMR studies on the energy metabolism of glial and neuronal cells. Dev Neurosci 1993;15:289–298. [PubMed: 7805581]

14. Akiyama H, Arai T, Kondo H, et al. Cell mediators of inflammation in the Alzheimer disease brain. Alzheimer Dis Assoc Disord 2000;14 (Suppl 1):S47–S53. [PubMed: 10850730]
15. Meda L, Baron P, Scarlato G. Glial activation in Alzheimer's disease: the role of Abeta and its associated proteins. Neurobiol Aging 2001;22:885–893. [PubMed: 11754995]
16. Miller BL, Moats RA, Shonk T, et al. Alzheimer disease: depiction of increased cerebral myo-inositol with proton MR spectroscopy. Radiology 1993;187:433–437. [PubMed: 8475286]
17. Moats RA, Ernst T, Shonk TK, et al. Abnormal cerebral metabolite concentrations in patients with probable Alzheimer disease. Magn Reson Med 1994;32:110–115. [PubMed: 8084225]
18. Martinez-Bisbal MC, Arana E, Marti-Bonmati L, et al. Cognitive impairment: classification by 1H magnetic resonance spectroscopy. Eur J Neurol 2004;11:187–193. [PubMed: 15009164]
19. Kantarci K, Jack CR Jr, Xu YC, et al. Regional metabolic patterns in mild cognitive impairment and Alzheimer's disease: a 1H MRS study. Neurology 2000;55:210–217. [PubMed: 10908893]
20. Kantarci K, Petersen RC, Boeve BF, et al. 1H MR spectroscopy in common dementias. Neurology 2004;63:1393–1398. [PubMed: 15505154]
21. Ernst T, Chang L, Melchor R, et al. Frontotemporal dementia and early Alzheimer disease: differentiation with frontal lobe H-1 MR spectroscopy. Radiology 1997;203:829–836. [PubMed: 9169712]
22. Chantal S, Braun CM, Bouchard RW, et al. Similar 1H magnetic resonance spectroscopic metabolic pattern in the medial temporal lobes of patients with mild cognitive impairment and Alzheimer disease. Brain Res 2004;1003:26–35. [PubMed: 15019560]
23. Catani M, Cherubini A, Howard R, et al. (1)H-MR spectroscopy differentiates mild cognitive impairment from normal brain aging. Neuroreport 2001;12:2315–2317. [PubMed: 11496102]
24. Shonk TK, Moats RA, Gifford P, et al. Probable Alzheimer disease: diagnosis with proton MR spectroscopy. Radiology 1995;195:65–72. [PubMed: 7892497]
25. Parnetti L, Tarducci R, Presciutti O, et al. Proton magnetic resonance spectroscopy can differentiate Alzheimer's disease from normal aging. Mech Ageing Dev 1997;97:9–14. [PubMed: 9223122]
26. Rose SE, de Zubicaray GI, Wang D, et al. A 1H MRS study of probable Alzheimer's disease and normal aging: implications for longitudinal monitoring of dementia progression. Magn Reson Imaging 1999;17:291–299. [PubMed: 10215485]
27. Soher BJ, Vermathen P, Schuff N, et al. Short TE in vivo (1)H MR spectroscopic imaging at 1.5 T: acquisition and automated spectral analysis. Magn Reson Imaging 2000;18:1159–1165. [PubMed: 11118771]
28. Posse S, DeCarli C, Le Bihan D. Three-dimensional echo-planar MR spectroscopic imaging at short echo times in the human brain. Radiology 1994;192:733–738. [PubMed: 8058941]
29. Kapeller P, McLean MA, Griffin CM, et al. Preliminary evidence for neuronal damage in cortical grey matter and normal appearing white matter in short duration relapsing-remitting multiple sclerosis: a quantitative MR spectroscopic imaging study. J Neurol 2001;248:131–138. [PubMed: 11284131]
30. Mueller SG, Laxer KD, Suhy J, et al. Spectroscopic metabolic abnormalities in mTLE with and without MRI evidence for mesial temporal sclerosis using hippocampal short-TE MRSI. Epilepsia 2003;44:977–980. [PubMed: 12823584]
31. Simister RJ, Woermann FG, McLean MA, et al. A short-echo-time proton magnetic resonance spectroscopic imaging study of temporal lobe epilepsy. Epilepsia 2002;43:1021–1031. [PubMed: 12199727]
32. Durazzo TC, Gazdzinski S, Banys P, et al. Cigarette smoking exacerbates chronic alcohol-induced brain damage: a preliminary metabolite imaging study. Alcohol Clin Exp Res 2004;28:1849–1860. [PubMed: 15608601]
33. Auer DP, Schirmer T, Heidenreich JO, et al. Altered white and gray matter metabolism in CADASIL: a proton MR spectroscopy and 1H-MRSI study. Neurology 2001;56:635–642. [PubMed: 11245716]
34. Block W, Traber F, Kuhl CK, et al. 1H-MR spectroscopic imaging in patients with clinically diagnosed Alzheimer's disease. Rofo Fortschr Geb Rontgenstr Neuen Bildgeb Verfahr 1995;163:230–237. [PubMed: 7548870]
35. Colla M, Ende G, Bohrer M, et al. MR spectroscopy in Alzheimer's disease: gender differences in probabilistic learning capacity. Neurobiol Aging 2003;24:545–552. [PubMed: 12714111]

36. Mielke R, Schoppho HH, Kugel H, et al. Relation between 1H MR spectroscopic imaging and regional cerebral glucose metabolism in Alzheimer's disease. Int J Neurosci 2001;107:233–245. [PubMed: 11328693]
37. Tedeschi G, Bertolino A, Lundbom N, et al. Cortical and subcortical chemical pathology in Alzheimer's disease as assessed by multislice proton magnetic resonance spectroscopic imaging. Neurology 1996;47:696–704. [PubMed: 8797467]
38. Chao LL, Schu N, Kramer JH, et al. Reduced medial temporal lobe N-acetyl aspartate in cognitively impaired but nondemented patients. Neurology 2005;64:282–289. [PubMed: 15668426]
39. Zhu XP, Young K, Ebel A, et al. Robust analysis of short echo time 1H MRSI of human brain. Magn Reson Med 2006;55:706–711. [PubMed: 16463345]
40. Zhu, XP.; Young, K.; Soher, JB., et al. New spectral analysis of short echotime multislice 1H MRSI in human brain using eigen spectra, baseline correction and frequency alignment; Proceedings of the 13th Annual Meeting of ISMRM; Miami Beach, USA. 2005. p. 55
41. Mungas D, Reed BR, Ellis WG, et al. The effects of age on rate of progression of Alzheimer disease and dementia with associated cerebrovascular disease. Arch Neurol 2001;58:1243–1247. [PubMed: 11493164]
42. McKhann G, Drachman D, Folstein M, et al. Clinical diagnosis of Alzheimer's disease: report of the NINCDS-ADRDA Work Group under the auspices of Department of Health and Human Services Task Force on Alzheimer's Disease. Neurology 1984;34:939–944. [PubMed: 6610841]
43. Folstein MF, Folstein SE, McHugh PR. "Mini-mental state". A practical method for grading the cognitive state of patients for the clinician. J Psychiatr Res 1975;12:189–198. [PubMed: 1202204]
44. Wiedermann D, Schuff N, Matson GB, et al. Short echo time multislice proton magnetic resonance spectroscopic imaging in human brain: metabolite distributions and reliability. Magn Reson Imaging 2001;19:1073–1080. [PubMed: 11711231]
45. Haupt CI, Schuff N, Weiner MW, et al. Removal of lipid artifacts in 1H spectroscopic imaging by data extrapolation. Magn Reson Med 1996;35:678–687. [PubMed: 8722819]
46. Soher BJ, Young K, Govindaraju V, et al. Automated spectral analysis III: application to in vivo proton MR spectroscopy and spectroscopic imaging. Magn Reson Med 1998;40:822–831. [PubMed: 9840826]
47. MacKay S, Ezekiel F, Di Sclafani V, et al. Alzheimer disease and subcortical ischemic vascular dementia: evaluation by combining MR imaging segmentation and H-1 MR spectroscopic imaging. Radiology 1996;198:537–545. [PubMed: 8596863]
48. Jack CR Jr, Petersen RC, Xu Y, et al. Rate of medial temporal lobe atrophy in typical aging and Alzheimer's disease. Neurology 1998;51:993–999. [PubMed: 9781519]
49. Andreasen NC, Rajarethinam R, Cizadlo T, et al. Automatic atlas-based volume estimation of human brain regions from MR images. J Comput Assist Tomogr 1996;20:98–106. [PubMed: 8576490]
50. Pinheiro, JC.; Bates, DM. Mixed-effects Models in S and S-PLUS. New York: Springer; 2000.
51. Chetelat G, Baron JC. Early diagnosis of Alzheimer's disease: contribution of structural neuroimaging. Neuroimage 2003;18:525–541. [PubMed: 12595205]
52. Kantarci K, Jack CR Jr. Neuroimaging in Alzheimer disease: an evidence-based review. Neuroimaging Clin N Am 2003;13:197–209. [PubMed: 13677801]
53. Schu N, Capizzano AA, Du AT, et al. Different patterns of N-acetyl aspartate loss in subcortical ischemic vascular dementia and AD. Neurology 2003;61:358–364. [PubMed: 12913198]
54. Choi CG, Frahm J. Localized proton MRS of the human hippocampus: metabolite concentrations and relaxation times. Magn Reson Med 1999;41:204–207. [PubMed: 10025631]
55. Waldman AD, Rai GS, McConnell JR, et al. Clinical brain proton magnetic resonance spectroscopy for management of Alzheimer's and sub-cortical ischemic vascular dementia in older people. Arch Gerontol Geriatr 2002;35:137–142. [PubMed: 14764351]
56. Heun R, Schlegel S, Graf-Morgenstern M, et al. Proton magnetic resonance spectroscopy in dementia of Alzheimer type. Int J Geriatr Psychiatry 1997;12:349–358. [PubMed: 9152720]
57. Stoppe G, Bruhn H, Pouwels PJ, et al. Alzheimer disease: absolute quantification of cerebral metabolites in vivo using localized proton magnetic resonance spectroscopy. Alzheimer Dis Assoc Disord 2000;14:112–119. [PubMed: 10850750]

58. Brun A. Frontal lobe degeneration of non-Alzheimer type. I. Neuropathology. Arch Gerontol Geriatr 1987;6:193–208. [PubMed: 3689053]
59. Neary D, Snowden JS, Northen B, et al. Dementia of frontal lobe type. J Neurol Neurosurg Psychiatry 1988;51:353–361. [PubMed: 3258902]
60. Lien YH, Shapiro JI, Chan L. Effects of hypernatremia on organic brain osmoles. J Clin Invest 1990;85:1427–1435. [PubMed: 2332498]
61. De Stefano N, Narayanan S, Francis GS, et al. Evidence of axonal damage in the early stages of multiple sclerosis and its relevance to disability. Arch Neurol 2001;58:65–70. [PubMed: 11176938]
62. Vermathen P, Laxer KD, Matson GB, et al. Hippocampal structures: anteroposterior N-acetyl aspartate differences in patients with epilepsy and control subjects as shown with proton MR spectroscopic imaging. Radiology 2000;214:403–410. [PubMed: 10671587]
63. Li BS, Babb JS, Soher BJ, et al. Reproducibility of 3D proton spectroscopy in the human brain. Magn Reson Med 2002;47:439–446. [PubMed: 11870829]
64. Klunk WE, Xu C, Panchalingam K, et al. Quantitative 1H and 31P MRS of PCA extracts of postmortem Alzheimer's disease brain. Neurobiol Aging 1996;17:349–357. [PubMed: 8725895]
65. Fernandez A, Garcia-Segura JM, Ortiz T, et al. Proton magnetic resonance spectroscopy and magnetoencephalographic estimation of delta dipole density: a combination of techniques that may contribute to the diagnosis of Alzheimer's disease. Dement Geriatr Cogn Disord 2005;20:169–177. [PubMed: 16020946]
66. Dixon RM, Bradley KM, Budge MM, et al. Longitudinal quantitative proton magnetic resonance spectroscopy of the hippocampus in Alzheimer's disease. Brain 2002;125:2332–2341. [PubMed: 12244089]
67. Kantarci K, Xu Y, Shiung MM, et al. Comparative diagnostic utility of different MR modalities in mild cognitive impairment and Alzheimer's disease. Dement Geriatr Cogn Disord 2002;14:198–207. [PubMed: 12411762]
68. Antuono PG, Jones JL, Wang Y, et al. Decreased glutamate+glutamine in Alzheimer's disease detected in vivo with (1)H-MRS at 0.5T. Neurology 2001;56:737–742. [PubMed: 11274307]

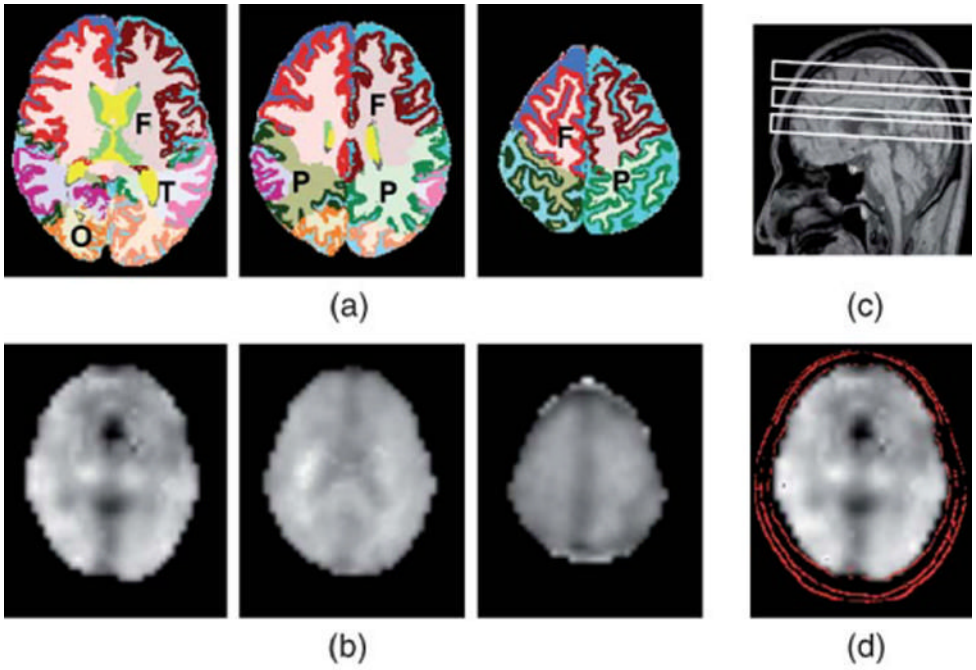

FIGURE 1.

A, Segmented MRI showing frontal (F), parietal (P), temporal (T), or occipital (O) lobe. WM, GM, and CSF were rendered with different colors; B, Transaxial NAA images; C, A sagittal scout MRI indicating slice positions; D, A contour plot showing alignment of MRI and MRSI.

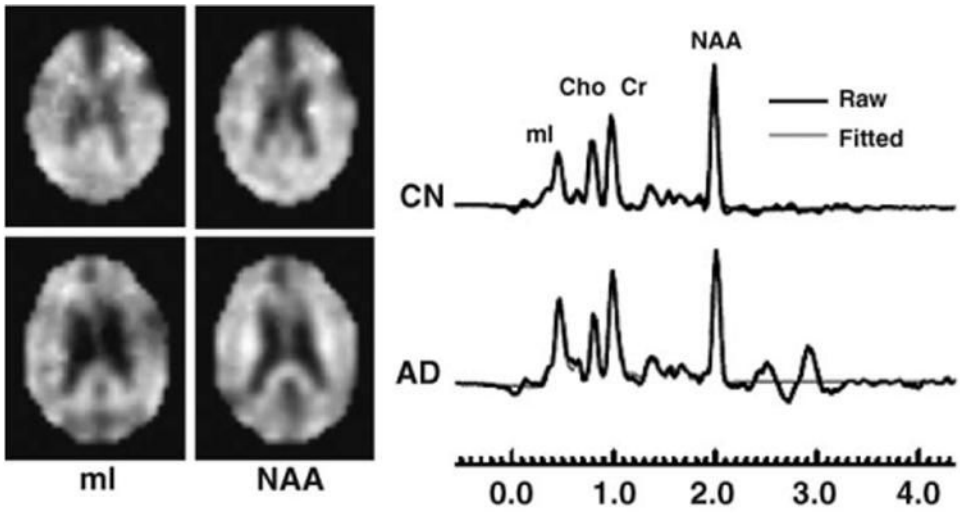

FIGURE 2.
Example of mI and NAA images and RCMS from MRSI voxel in the regions of parietal GM in a 66-year-old AD and an 85-year-old CN.

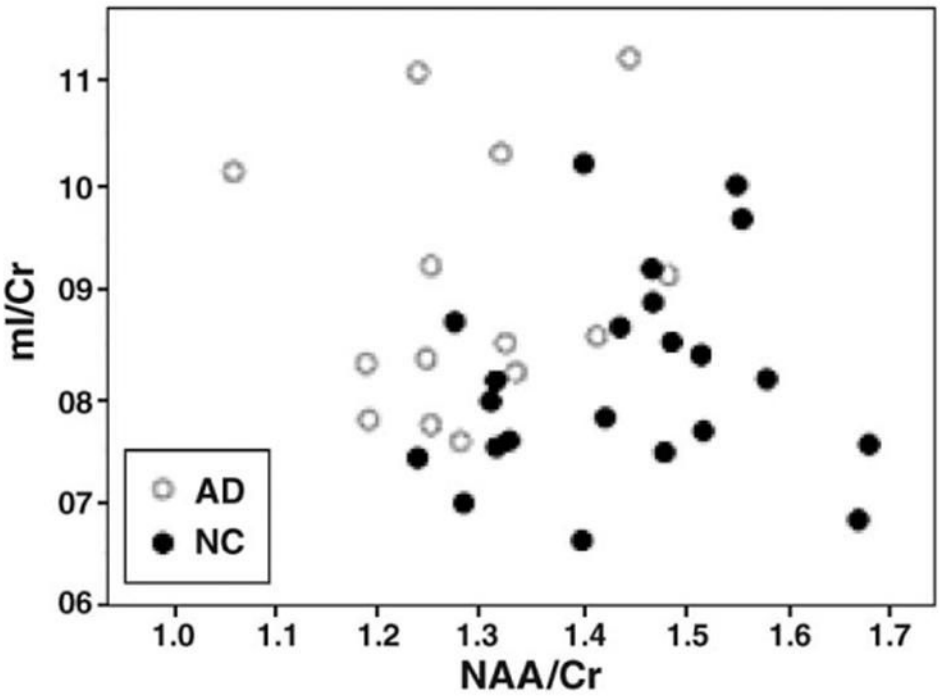

FIGURE 3.
mI/Cr in parietal lobe GM plotted against NAA/Cr from each of 14 AD (○) and 22 CN (●) measured from short TE MRSI.

TABLE 1

Subject Demographics

Characteristics	CN	AD
N (% Female)	22 (57)	14 (59)
Age (y)	72.1±8.5	70.6±7.2
MMSE score	29.7±0.5 (N=11)	20.0±6.7(N=13) *†
MMSE score range	29 to 30	8 to 28
WMH (cm^3)	4.36±6.51	2.42±1.62

Data represented as mean±standard deviation.

* $P<0.0001$ between CN and AD for 2-sided *t* test.

† Number of cases, who had MMSE scores.

TABLE 2

Hippocampal, Cortical GM Volume (cm^3)[†] From Structural MRI in AD (N = 14) and CN (N = 22)

	CN	AD	% Differences (%)	*P*[*]
Right hippocampus	2.34±0.28	1.82±0.21	−22.2	<0.0001
Left hippocampus	2.32±0.32	1.81±0.22	−22.0	<0.0001
Cortical GM	593.0±32.4	550.7±25.9	−7.1	=0.0002
WM	508.6±40.1	483.1±34.4	−5.0	=0.02

[*] *P* values are for multivariate analysis of covariance using an LME model.

[†] Volumes, expressed as mean±SD, have been normalized to intracranial volume and scaled to the mean intracranial volume of all subjects to maintain volume in units of cm^3.

TABLE 3

Raw Data Summaries: NAA and mI Concentrations and Selected Metabolite Ratios of Parietal GM, Frontal GM, Parietal WM, and Frontal WM in AD (N = 14) and CN (N = 22)

	Metabolites	AD Mean±SD	CN Mean±SD	% Difference (%)	*P**
Parietal GM	NAA	2.00±0.30	2.22±0.26	−10.0	0.044
	mI	1.39±0.19	1.26±0.18	10.3	0.048
	NAA/Cr	1.28±0.11	1.44±0.12	−11.1	0.0009
	mI/Cr	0.90±0.12	0.82±0.10	9.8	0.07
	NAA/mI	1.45±0.21	1.78±0.25	−18.5	0.0003
Frontal GM	NAA	2.01±0.25	2.05±0.28	−2.0	0.68
	mI	1.47±0.35	1.26±0.19	16.7	0.40
	NAA/Cr	1.27±0.11	1.39±0.12	−8.6	0.006
	mI/Cr	0.94±0.22	0.86±0.10	9.3	0.93
	NAA/mI	1.41±0.25	1.64±0.23	−14.0	0.32
Parietal WM	NAA	2.40±0.24	2.51±0.25	−4.4	0.31
	mI	1.58±0.27	1.46±0.18	8.2	0.26
	NAA/Cr	1.49±0.11	1.61±0.13	−7.4	0.02
	mI/Cr	0.98±0.13	0.94±0.11	4.3	0.16
	NAA/mI	1.54±0.20	1.73±0.22	−11.0	0.03
Frontal WM	NAA	2.44±0.31	2.45±0.30	−0.4	0.72
	mI	1.41±0.26	1.41±0.17	0.0	0.97
	NAA/Cr	1.48±0.11	1.54±0.14	−3.9	0.12
	mI/Cr	0.86±0.13	0.88±0.09	−2.3	0.47
	NAA/mI	1.77±0.31	1.75±0.21	1.1	0.93

* *P* values are for multivariate analysis of covariance using an LME model.

TABLE 4

Classification of Patients With AD and CN Subjects

	Overall Classification (%)	Sensitivity (%)	Specificity (%)	AUC (Mean ±SE)	*P*
NAA/Cr	67	57	73	0.81±0.06	0.010
NAA/Cr+mI/Cr	78	64	86	0.90±0.05	0.010, 0.039
NAA/mI	75	57	86	0.86±0.04	0.013
Hippocampus	81	71	86	0.94±0.04	0.005
Hippocampus+NAA/mI	89	86	91	0.97±0.03	0.020, 0.098

Sensitivity, specificity, and overall correct classification were obtained from a leave-one-out procedure based on logistic regression analyses. A uniform cutoff value of 0.5 was used for each set of sensitivity and specificity. Mean values and standard errors (SE) of area under the receiver operator curves (AUC) were calculated by bootstrapping a general linear model. All *P* values were obtained from the logistic regression analyses. For models with combinations of explanatory variables, the *P* values associated with each variable were listed on separate lines.

TABLE 5

Comparison of Literature Values of Classification Between AD and CN Using MRSI or SV MRS

Authors	Classification (%)			Metabolites (Brain Lobe)	MRS Method
	Overall Classification	Sensitivity	Specificity		
Fernandez et al, 2005[65]	90 (n=20)	90	90	mI/NAA (Temporo-parietal)	SV M RSTE=35ms
Schuff et al, 2002[10]	83 (n=110)	84	83	NAA (Medial temporal)	MRSI TE=135 ms
Dixon et al, 2002[66]	68–70 (n=25)	NA	NA	NAA (Hippocampus)	SV MRS TE=90ms
Kantarci et al, 2002[67]	NA (n=83)	82	80	NAA/ mI (Posterior cingulate)	SV MRS TE=30ms
Antuono et al, 2001[68]	80 (n=30)	NA	NA	mI/Cr+NAA/ Cr (Posterior cingulate)	SV MRS TE=68ms
Mackay et al, 1996[47]	82 (n=20)	100	73	NAA/ Cho (Posterior mesial)	PRESS MRSI TE=272 ms
Shonk et al, 1995[24]	NA (n=97)	83	98	NAA/mI (Occipital)	SV MRS TE=30ms